

Strongly Anisotropic Electronic Transport at Landau Level Filling Factor $\nu = 9/2$ and $\nu = 5/2$ Under Tilted Magnetic Field

W. Pan^{a,b}, R.R. Du^{c,b}, H.L. Stormer^{d,e}, D.C. Tsui^a, L.N. Pfeiffer^d, K.W. Baldwin^d, and K.W. West^d

a) Dept. Electr. Eng., Princeton University, Princeton, NJ

b) NHMFL, Tallahassee, FL

c) Dept. Phys., University of Utah, Salt Lake City, UT

d) Bell Labs, Lucent Technologies, Bell Laboratories, Murray Hill, NJ

e) Dept. Phys. and Dept. Appl. Phys., Columbia University, New York, NY

(August 9, 2018)

We have investigated the influence of an increasing in-plane magnetic field on the states at half-filling of Landau levels ($\nu = 11/2, 9/2, 7/2$, and $5/2$) of a two-dimensional electron system. In the electrically anisotropic phase at $\nu = 9/2$ and $11/2$ an in-plane magnetic field of ~ 1 - 2 T overcomes its initial pinning to the crystal lattice and *reorient* this phase. In the initially isotropic phases at $\nu = 5/2$ and $7/2$ an in-plane magnetic field *induces* a strong electrical anisotropy. In all cases, for high in-plane fields, the high resistance axis is parallel to the direction of the in-plane field.

The electrical transport properties at half-filling of either spin state of Landau levels of a two-dimensional electron system (2DES) have turned out to be very diverse. In the lowest Landau level (filling factor $\nu < 2$) at half-filling of the down-spin level ($\nu = 1/2$) and at half-filling of the up-spin level ($\nu = 3/2$) the Hall resistance, R_H , is linear in magnetic field, B , and the magneto resistance, R , is only weakly temperature dependent [1]. Today, this behavior is interpreted as the formation of composite fermions (CFs) that fill up a fermi sea to a fixed fermi wave vector, k_F , and the cancellation of the externally applied magnetic field [2,3].

In the second Landau level ($4 < \nu < 2$) at half-filling of the down-spin level ($\nu = 5/2$) and half filling of the up-spin level ($\nu = 7/2$) the Hall resistance shows a plateau and the magneto resistance exhibits the deep minimum of the fractional quantum Hall effect (FQHE) [4]. The occurrence of a FQHE state at such an *even*-denominator filling is puzzling, since from simple symmetry requirements on the wave function, one would have expected the FQHE to occur only at *odd*-denominator filling [5]. The origin of this even-denominator FQHE remains mysterious, but is now conjectured to arise from the formation of CF pairs that condense into a novel state [6–8].

In higher Landau levels ($\nu > 4$) at half-filling of either spin level ($\nu = 9/2, 11/2, 13/2, 15/2$) the Hall resistance, R_H , is erratic and R exhibits a strongly anisotropic behavior, showing a strong peak in one current direction (R_{xx}) and a deep minimum when the current direction is rotated by 90° within the plane (R_{yy}) [9–11]. The origin of these states remain also unclear. They are believed to arise from the formation of a striped electronic phase [12,13] or an electronic phase akin to a liquid crystal phase [14]. The broken symmetry is speculated to arise from a slight misalignment of the crystallographic direction of the GaAs/AlGaAs host lattice, which pins the phase [10,11]. The wealth of different behaviors makes the states at half-filling presently one of the most fascinating topics in 2D electron physics in a high magnetic

field.

Tilting the magnetic field with respect to the sample normal is a classical method to gently alter the conditions for the 2DES [15]. In an ideal 2DES a tilted magnetic field does not modify the orbital motion but only the Zeeman splitting of its spin level. In a real 2DES, which has a finite thickness of $\sim 100\text{\AA}$, the orbital motion is affected only to second order. Measuring the influence of such a tilt on the transport parameters often allows to narrow down the range of possible underlying electronic states.

Such measurements have been performed extensively on the standard odd-denominator FQHE states [16] as well as on the half-filling states at $\nu = 1/2, 3/2, 5/2$, and $7/2$ [17,18]. The interpretation of the data largely draws from the increase of the Zeeman energy under tilt. Such experiments have been instrumental in supporting and expanding the CF model around $\nu = 1/2$ and $3/2$ [19,20] and they suggest the involvement of the spin-degree of freedom in the formation of the states at $\nu = 5/2$ and $7/2$ [18]. For higher Landau levels such angular-dependent measurements have not yet been performed. Moreover, the in-plane anisotropy of the resistance in this filling factor regime introduces a new variable into such tilt experiments.

Previous tilt experiments in the regime of the FQHE always assumed that only the angle of the magnetic field with respect to the sample normal mattered to the transport behavior, whereas the azimuth of the field, *i.e.* the direction of the so-created in-plane magnetic field (B_{ip}), was immaterial. While this implicit assumption should always have been suspect, since the in-plane current direction breaks the planar isotropy, it obviously needs to be investigated and justified in the case of the $\nu = 9/2, 11/2$ states, which show strongly anisotropic phases. In its extremes, the B -field can be tilted towards the direction that shows the maximum in R (R_{xx} , hard direction) and towards the direction that shows the minimum in R (R_{yy} , easy direction), which is rotated with respect to

R_{xx} by approximately 90° within the plane of the sample.

We have performed such tilt experiments on the states at half-filling and observed very different behavior for different states. For the states at $\nu = 9/2$ and $11/2$ the initial direction of the in-plane anisotropy is overwritten by the in-plane field. Depending on the tilt direction, and therefore the direction of the in-plane field, the easy direction and the hard direction either remain in place or trade places with increasing B_{ip} . More surprisingly yet, the $\nu = 5/2$ and $7/2$ states, which *do not show* any initial in-plane anisotropy become strongly anisotropic under tilt, to a degree similar as the states at $\nu = 9/2$ and $\nu = 11/2$. In all cases, under high tilt angles, it is exclusively the relative direction of current (I) and in-plane magnetic field (B_{ip}), that determines whether R shows a minimum or a maximum. More specifically, in the large in-plane limit, R is a deep minimum when measured *perpendicular* to the in-plane magnetic field and it exhibits a strong maximum when measured *parallel* to the in-plane field. At the same time, neither the half-filled states in the lowest Landau levels ($\nu = 1/2$ and $3/2$) nor any of the FQHE states in their vicinity show such anisotropies. The origin of the effect that an in-plane magnetic field exerts onto the states at half-filling remains unclear.

Our sample consists of a modulation-doped GaAs/AlGaAs heterostructure which has a 2DES with an electron density of $2.2 \times 10^{11} \text{ cm}^{-2}$ and a low-temperature mobility of $\mu = 1.7 \times 10^7 \text{ cm}^2/\text{V sec}$. The specimen is similar to the one used in our previous, un-tilted experiments [11] on the $\nu = 9/2$ and $11/2$ states, but has a yet higher mobility. The size of the sample is about $4 \text{ mm} \times 4 \text{ mm}$ with eight indium contacts placed symmetrically around the edges, four at the sample corners and four in the center of the four edges. The sample is placed on a precision rotator inside the mixing chamber of a dilution refrigerator placed within a superconducting magnet. The equipment reaches a base temperature of 40 mK in magnet fields up to $B = 18 \text{ T}$. The sample can be rotated *in-situ* around an axis perpendicular to the field from $\theta = 0^\circ$ to $\theta = 90^\circ$. Experiments are performed at fixed angle θ while sweeping B . Since for our sample of fixed electron density only the magnetic field perpendicular to the 2DES ($B_{perp} = B \times \cos(\theta)$) determines the filling factor ν , we plot our data against B_{perp} . At any given angle θ the in-plane field ($B_{ip} = B \times \sin(\theta)$) is then proportional to the perpendicular magnetic field, *i.e.* $B_{ip} = B_{perp} \times \tan(\theta)$. With a total magnetic field of 18 T available and an electron density of $2.2 \times 10^{11} \text{ cm}^{-2}$, which requires a B_{perp} of $\sim 3.6 \text{ T}$ to reach the $\nu = 5/2$ state, the sample can be tilted as much as $\theta = \arccos(3.6\text{T}/18\text{T}) \approx 78^\circ$. This creates an in-plane magnetic field as high as $B_{ip} = B_{perp} \times \tan(78^\circ) \approx 17 \text{ T}$.

The sample was mounted in two different configurations onto the rotator. In the first instance, the axis of rotation was along y , the easy direction (low resistance) of the $9/2$ and $11/2$ states, allowing to place increasing B_{ip} along the hard direction (high resistance) (see inserts top Fig. 2). In the second instance, the axis of rotation ran

along x , the hard direction (high resistance) of the $9/2$ and $11/2$ states, allowing to place increasing B_{ip} along the easy direction (low resistance) (see inserts bottom Fig. 2). Since the hard and easy direction are not very precisely defined within the plane, but only known to run roughly along the edges of the square sample, the in-plane field in our experiment may not run precisely along either the hard or the easy direction, but it will run predominantly in such a direction. Transport experiments were performed using standard 7 Hz look-in techniques at a current of 5 nA which is known from previous experiments [11] on these samples to cause negligible electron heating. The transport anisotropy was measured at 14 different angles between $\theta = 0^\circ$ and $\theta = 78^\circ$ in both configurations. The angle θ was determined from the orderly $\cos(\theta)$ shift of several strong minima of the FQHE.

Fig. 1 shows an overview over R_{xx} and R_{yy} at zero-tilt ($B_{perp} = B$, $B_{ip} = 0$). The well-documented strong anisotropy of the $\nu = 9/2$, $11/2$, $13/2$, and $15/2$ states is apparent in the data. States at filling factor $\nu < 4$ show negligible anisotropy. Any residual difference between R_{xx} and R_{yy} in this regime can be attributed to a slight difference in the geometry of the contact arrangement for both measurements. In the following tilt experiments we will focus on the states at $\nu = 9/2$ and $11/2$ as well as $\nu = 5/2$ and $7/2$. The states at half-filling of the next higher Landau level, $\nu = 13/2$ and $15/2$ show behavior similar to the $\nu = 9/2$ and $11/2$ states, although less well pronounced.

Fig. 2 shows R_{xx} and R_{yy} data for $6 > \nu > 2$ at selected tilt angles, θ . The data of the top panels (Fig. 2a,b) are taken with B_{ip} pointing along the *hard* direction, x , of the anisotropic state, whereas the data of the bottom panel (Fig. 2c,d) are taken for B_{ip} along the *easy* direction, y , of the anisotropic state. The inserts depicts the geometries. The behavior of R_{xx} and R_{yy} as a function of tilt differs dramatically between the upper and the lower panels.

For $\nu = 9/2$ and $11/2$ in the absence of tilt ($\theta = 0.0^\circ$), the traces for R_{xx} (solid lines in Fig. 2a and Fig. 2c) and the traces for R_{yy} (dotted lines in Fig. 2a and Fig. 2c) are essentially identical. This reinforces our assertion, that cycling of the sample to room temperature, necessary to change the sample configuration, has negligible effect on the transport features. As the sample is tilted toward $\theta = 74.3^\circ$ the R_{xx} and the R_{yy} traces behave very differently in both panels. When B_{ip} is increased along the *hard* direction (Fig. 2a) R_{xx} is somewhat reduced in amplitude but recovers at the highest tilt angles while R_{yy} lifts up only slightly from its value at $\theta = 0^\circ$. Nevertheless, the maximum remains a maximum and the minimum remains a minimum. On the other hand, when B_{ip} is increased along the *easy* direction (Fig. 2c) R_{xx} collapses and develops into a minimum, while R_{yy} rises and becomes a maximum at the highest tilt. Here maximum and minimum *trade places*. At the highest angles the shape of R_{yy} in Fig. 2c practically equals R_{xx} in Fig. 2a and vice versa.

For $\nu = 5/2$ and $7/2$, in the absence of tilt, the data show practically no anisotropy. For this $\theta = 0^\circ$ situation, R_{xx} and R_{yy} are very similar within Fig. 2b and both are very similar within Fig. 2d. However, tilting of the sample and the associated increase of B_{ip} drastically alters the data and introduces a strong anisotropy between R_{xx} and R_{yy} . As B_{ip} increases along the x-direction (Fig. 2b), R_{xx} increases, while R_{yy} decreases. On the other hand, as B_{ip} increases along the y-direction (Fig. 2d), R_{xx} decreases, while R_{yy} increases. The hard direction always develops *along* B_{ip} , whereas the easy direction always runs *perpendicular* to B_{ip} . This means that, the directionality of this anisotropy is determined by the direction of B_{ip} . This is particularly apparent at the highest angle shown, $\theta = 74.3^\circ$, where R_{xx} and R_{yy} seem to have traded places when going from Fig. 2b to Fig. 2d. Furthermore, at such large angles the anisotropy in the $\nu = 5/2$ and $7/2$ states becomes similar to the anisotropy in the $\nu = 9/2$ and $11/2$ states. Independent of the starting conditions at $\theta = 0^\circ$, eventually the direction of B_{ip} governs the directionality of the anisotropy for all such states at $\nu = 11/2, 9/2, 7/2$, and $5/2$. On the other hand, no such anisotropy — neither preexisting nor induced — is found at $\nu = 3/2$ nor at $\nu = 1/2$ in the lowest Landau level in tilted magnetic field (not shown). This observation seems to link the states at $\nu = 11/2$ and $9/2$ with the states at $\nu = 7/2$ and $5/2$. Beyond the equivalence in their high-angle anisotropy, even the general shape of R_{xx} and R_{yy} approach each other at such high angles.

Fig. 3 summarizes the anisotropies for the strongest of states at $\nu = 9/2$ and $\nu = 5/2$. The four top panels (Fig. 3a,b,c,d) match the four panels of Fig. 2a,b,c,d. They show the amplitudes of R_{xx} (solid line) and R_{yy} (dotted line) at $\nu = 9/2$ and $\nu = 5/2$ filling versus the strength of the in-plane magnetic field. The bottom panels of Fig. 3 represent the anisotropies of the $\nu = 9/2$ state and the $\nu = 5/2$ state as calculated from the panels above.

For $\nu = 9/2$, when B_{ip} increases along the x-direction (Fig. 3a) the amplitude of R_{xx} parallel to B_{ip} , drops rapidly by more than a factor of two, reaches a minimum strength at $B_{ip} \sim 2$ T and then recovers at the highest fields to about 70% of its original value. The amplitude of the R_{yy} , perpendicular to B_{ip} , rises somewhat from zero, reaches a shallow maximum also at $B_{ip} \sim 2$ T, and decays slightly for higher fields.

On the other hand, when B_{ip} increases along the y-direction (Fig. 3c) the amplitude of R_{xx} perpendicular to B_{ip} , collapses precipitously, almost touching zero at $B_{ip} \sim 1$ T and remains at about 5% of its original value for all higher in-plane fields. The amplitude of R_{yy} , parallel to B_{ip} , rises dramatically from zero over the same, initial field range, reaches a value of about half of the initial R_{xx} and increases somewhat beyond this level for higher in-plane fields. The amplitudes of R_{xx} and R_{yy} obviously trade places in Fig. 3c, while R_{xx} always exceeds R_{yy} in Fig. 3a. However, the initial behavior for $B_{ip} \lesssim 1$ T is very similar for R_{xx} and R_{yy} in both panels

and the behavior is similar again for $B_{ip} \gtrsim 2$ T albeit R_{xx} and R_{yy} having traded places in Fig. 3c in the interim regime. In fact, disregarding the narrow field region of the minimum in panel a) and crossing in panel b), the general pattern exhibited by the data of both panels is remarkably similar.

For $\nu = 5/2$ in Fig. 3b and 3d, the amplitudes of R_{xx} and R_{yy} are essentially identical for $B_{ip} = 0$ but they separate as B_{ip} increases. The order of R_{xx} and R_{yy} reflects the order of R_{xx} and R_{yy} in the high-field region of $\nu = 9/2$ in Fig. 3a and 3c. However, the separation of R_{xx} from R_{yy} is gradual and lacks any sharp transition regime.

The top four panels of Fig. 3 are further summarized in the bottom panels, which show the in-plane anisotropy parameter for $\nu = 9/2$ (Fig. 3e) and for $\nu = 5/2$ (Fig. 3f) as a function of B_{ip} for both in-plane directions. We define the anisotropy parameter as the ratio of the difference in amplitudes divided by their sum. The solid circles refers to B_{ip} along the x-direction, the open circles refers to B_{ip} along the y-direction, as depicted by the abbreviated insets next to the traces. This panel shows very clearly that for $\nu = 9/2$ an in-plane magnetic field along the originally hard direction, x, largely *preserves* the directional anisotropy, whereas an in-plane magnetic field along the originally easy direction, y, *reverses* the direction of anisotropy. An in-plane field of $B_{ip} \sim 1$ T - 2 T is sufficient to invert the anisotropy, *i.e.* rotate the underlying electronic state by $\sim 90^\circ$ in the plane. The $\nu = 5/2$ state, on the other hand, starts out isotropic and gradually develops an anisotropy whose directionality at large B_{ip} is similar in extend to the one of $\nu = 9/2$ in the neighboring panel.

At present the nature of the state at $\nu = 9/2$ (as well as $11/2, 13/2, 15/2, \dots$) remains unresolved. Electronic states akin to a charge density wave [12,13] or a liquid crystal state [14] are being proposed, which would give rise to anisotropic transport in the plane of the 2DES. Earlier experiments on the anisotropy of R in perpendicular magnetic field found the hard and easy direction of transport to be pinned to the lattice of the sample. This spontaneous symmetry breaking is conjectured to arise from a slight misalignment of the GaAs/AlGaAs interface with respect to the [100] direction of the crystal, which causes mono-atomic steps at the interface in a particular direction within the plane [10,11]. The electronic phase at half-filling in these higher Landau levels is believed to align itself with respect to these steps, leading to anisotropic transport in a given direction.

Our data in tilted magnetic fields indicate that this initial pinning of the anisotropic electronic phase can be overcome by an in-plane magnetic field of $B_{ip} \sim 1$ T - 2 T. For fields higher than this value the directionality of the anisotropic phase is governed by the direction of the in-plane magnetic field. A resistance measurement with the current flowing parallel to this in-plane field always generates a maximum in R at $\nu = 9/2$ and equivalent states, whereas such a measurement performed with the

current flowing perpendicular to the in-plane field generates a minimum in R at $\nu = 9/2$ and equivalent states. The actual angular dependencies of the amplitudes of R (Fig. 3a,c) are rather non-monotonic and worth noting.

Let us assume a simple model of an electrically anisotropic phase with a preferential direction initially along one of the sample edges and eventually along the in-plane field. In Fig. 3c these directions are at 90° with respect to each other and the phase flips orientation over a narrow field range. In Fig. 3a these directions are parallel to each other and no flip occurs, since the phase is already aligned in the favorable direction. Under such conditions one would assume R to be largely angular independent, or at most to vary gradually with angle. Yet R_{xx} drops rapidly, by a factor of two, for small B_{ip} in Fig. 3a. A slight misalignment of the initial phase with respect to the x-axis is not expected to have such a dramatic effect. We conclude that an explanation of the angular dependencies of R in Fig. 3a and Fig. 3c requires a more complex model than a rigidly and smoothly rotating electronic phase.

While the nature of the state at $\nu = 5/2$ also remains obscure, it is believed to be quite distinct from the state at $9/2$. For one, the former is a true FQHE state [4] with plateau formation in R_{xy} , whereas such a plateau seems to be absent for the latter. And secondly, dramatic anisotropies in electronic transport in purely perpendicular magnetic field were only observed for the states at $9/2$ and equivalent, whereas they were absent in the $5/2$ state. Our tilted field experiments demonstrate that anisotropies not unlike those of the $9/2$ state can be induced in the $5/2$ state at sufficiently high in-plane magnetic field. On the other hand, such anisotropies have not been observed for the states at $\nu = 3/2$ and $\nu = 1/2$.

The mechanism for the drastic influence of an in-plane magnetic field on the transport properties of the 2D system is unresolved. Any non-zero in-plane magnetic field increases the total magnetic field, B , and therefore increases the Zeeman energy, E_Z , since the spin experiences the full B and not only its perpendicular component. Such a variation in E_Z is known to cause angular dependent coincidences between orbital energy and spin energy leading to the disappearance and reappearance of energy gaps in the IQHE and FQHE and hence to a strong angular dependence of R . In fact, the earlier observed disappearance of the FQHE at $\nu = 5/2$ under tilted magnetic field was considered to be of such a spin origin. However, no spin mechanism has been brought forward that would create a macroscopic electrical anisotropy, such as in the $5/2$ -state under tilt, or provide a preferred direction for an existing anisotropic state such as at $\nu = 9/2$. At present we are not aware of a model for our observations.

We would like to thank E. Palm and T. Murphy for experimental assistance, and B. I. Altshuler and S. H. Simon for discussions. A portion of this work was performed at the National High Magnetic Field Laboratory which is supported by NSF Cooperative Agreement No. DMR-9527035 and by the State of Florida. D.C.T. and

W.P. are supported by NSF and by the DOE. R.R. Du is supported by NSF and by the Sloan Foundation.

-
- [1] H.-W. Jiang, H. L. Stormer, D. C. Tsui, L. N. Pfeiffer and K. W. West, Phys. Rev. B **40**, 12013 (1989).
 - [2] *Composite Fermions: A Unified View of the Quantum Hall Regime*, O. Heinonen, ed, World Scientific, Singapore, 1998
 - [3] *Perspectives in Quantum Hall Effects*, S. DasSarma and A. Pinczuk eds. Wiley and Sons, 1998
 - [4] R. L. Willett, J. P. Eisenstein, H. L. Stormer, D. C. Tsui, A. C. Gossard, and J. H. English, Phys. Rev. Lett. **59**, 1776 (1987).
 - [5] F. D. M. Haldane in: *The Quantum Hall Effect*, R. E. Prange and S. M. Girvin eds. Springer Verlag, 1987, p303.
 - [6] G. Moore, and N. Read, Nuclear Physics **B360**, 362 (1991).
 - [7] M. Greiter, X.-G. Wen, and F. Wilczek, Phys. Rev. Lett. **66**, 3205 (1991).
 - [8] R. Morf, Phys. Rev. Lett. **80**, 1505 (1998).
 - [9] H. L. Stormer, R. R. Du, D. C. Tsui, L. N. Pfeiffer, and K. W. West, Bull. Amer. Phys. Soc. **38**, 235 (1993).
 - [10] M. P. Lilly, K. B. Cooper, J. P. Eisenstein, L. N. Pfeiffer, and K. W. West, Phys. Rev. Lett. **82**, 394 (1999).
 - [11] R. R. Du, D. C. Tsui, H. L. Stormer, L. N. Pfeiffer, K. W. Baldwin, and K. W. West, Solid State Commun. **109**, 389 (1999).
 - [12] A. A. Koulikov, M. M. Fogler, and B. I. Shklovskii, Phys. Rev. Lett. **76**, 499 (1996).
 - [13] R. Moessner and J. T. Chalker, Phys. Rev. B **54**, 5006 (1996).
 - [14] E. Fradkin and S. A. Kivelson, cond-mat/9810148, to appear in Phys. Rev. B **59**, March 15 (1999).
 - [15] F. F. Fang and P. J. Stiles, Phys. Rev. **174**, 823 (1968).
 - [16] R. J. Haug, K. v. Klitzing, R. J. Nicholas, J. C. Maan, and G. Weimann, Phys. Rev. B **36**, 4528 (1987).
 - [17] D. A. Syphers and J. E. Furneaux, Solid State Commun. **65**, 1513 (1988).
 - [18] J. P. Eisenstein, R. L. Willett, H. L. Stormer, D. C. Tsui, A. C. Gossard, and J. H. English, Phys. Rev. Lett. **61**, 997 (1988).
 - [19] R.R. Du, A.S. Yeh, H.L. Stormer, D.C. Tsui, L.N. Pfeiffer, and K.W. West, Phys. Rev. Lett. **75**, 3926 (1995).
 - [20] P.J. Gee, F.M. Peters, J. Singleton, S. Uji, H. Aoki, C.T.B. Foxon, and J.J. Harris, Phys. Rev. B **55**, R14313 (1996).

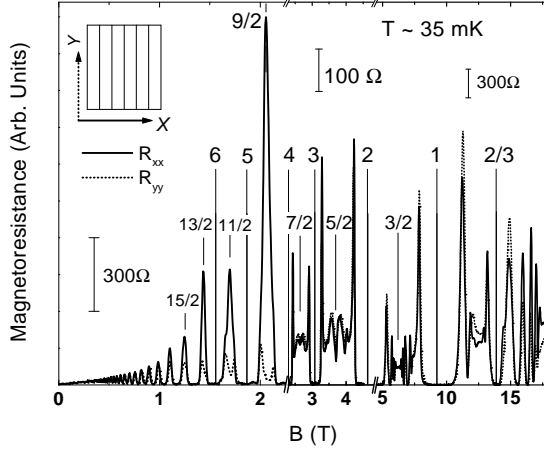


FIG. 1. Overview of magneto resistance of our high-mobility sample in perpendicular magnetic field. The features of the IQHE ($\nu = 1, 2, 3, \dots$) and FQHE ($\nu = 2/3$ etc) are clearly visible. Positions of half-filling are marked from $\nu = 3/2$ to $\nu = 15/2$. The insert shows the sample and the directions x and y . The magneto resistances R_{xx} and R_{yy} , taken in the x -direction and y -direction, respectively, in the plane are very similar except around half-filling of higher Landau levels ($\nu = 9/2$ to $\nu = 15/2$) where they strongly differ.

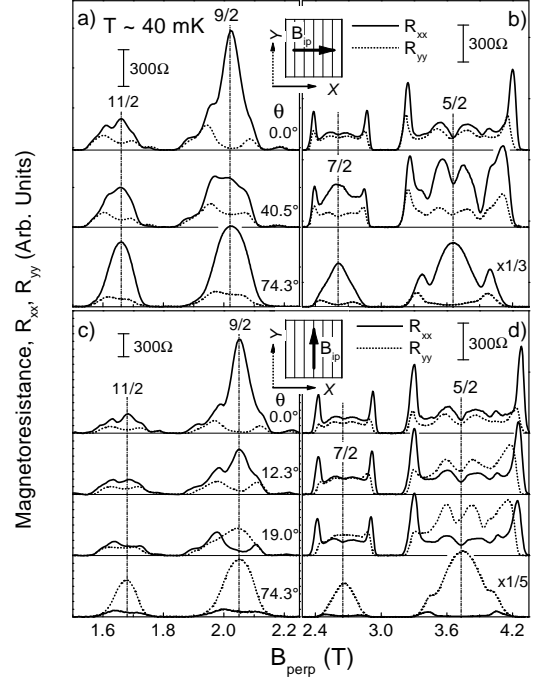


FIG. 2. Dependence of the magneto resistance R_{xx} and R_{yy} around filling factor $9/2$ and $11/2$ as well as around $5/2$ and $7/2$ on angle, θ , and direction of a tilted magnetic field, B . B_{perp} represents the field perpendicular to the sample, $B_{\text{perp}} = B \times \cos(\theta)$. The sample geometries are depicted as inserts. The x and y -directions are fixed with respect to the sample. Stripes in the sample indicate the initial anisotropy of the $9/2$ and $7/2$ state. In panel a) and b) the sample is rotated around the y -axis generating an increasing in-plane field $B_{ip} = B \times \sin(\theta)$ along the hard direction, x , whereas in panel c) and d) the sample is rotated around the x -axis generating an increasing B_{ip} along the easy direction, y .

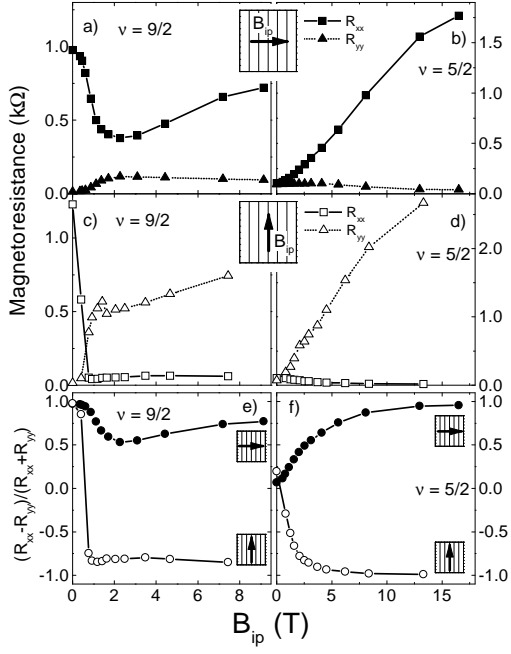


FIG. 3. Amplitudes of R_{xx} and R_{yy} at $\nu = 9/2$ and $\nu = 5/2$ as a function of in-plane magnetic field B_{ip} . The top four panels match the four panels of Fig. 2. Inserts depict the sample geometries. The bottom panels show the anisotropy factor determined from the amplitudes of the panels above, separate for the $9/2$ state (panel e)) and $5/2$ state (panel f)).